Research Article

Journal of PeptideScience

Received: 14 July 2009 Revised: 30 December 2009 Accepted: 15 January 2010 Published online in Wiley Interscience: 16 March 2010

(www.interscience.com) DOI 10.1002/psc.1216

Affinity of synthetic peptide fragments of MyoD for Id1 protein and their biological effects in several cancer cells

Chiu-Heng Chen,[a‡] Sheng-Chu Kuo,[b] Li-Jiau Huang,[b] Mei-Hua Hsu[b] and Feng-Di T. Lung[a*‡]

MyoD is a DNA-binding protein capable of specific interactions that involve the helix–loop–helix (HLH) domain. The HLH motif of MyoD can form oligomers with the HLH motif of Id1 (the inhibitor of DNA-binding proteins) that folds into a highly stable helical conformation stabilized by the self-association. The Id family consists of four related proteins that contain a highly conserved dimerization motif known as the HLH domain. In signaling pathways, Id proteins act as dominant negative antagonists of the basic helix–loop–helix (bHLH) family of transcription factors which play important roles in cellular development, proliferation, and differentiation. The mechanism of Id proteins is to antagonize bHLH proteins by binding as dominant negative HLH proteins to form high-affinity heterodimers with other bHLH proteins, thereby preventing them from binding to DNA and inhibiting transcription of differentiation-associated genes. The goal of this study is to design and synthesize peptide fragments of MyoD with high affinity for Id1 to interrupt the interactions among Id1, MyoD, and other bHLH DNA-binding proteins and to inhibit the proliferation of cancer cells. Affinity of each peptide for Id1 was determined by surface plasmon resonance (SPR) technology. The secondary structure of each peptide was studied by circular dichroism (CD) spectroscopy. Biological effects of each peptide in several cancer cells such as breast and colon cancer cells were analyzed. Results demonstrated that the peptide 3C (H-Tyr-Ile-Glu-Gly-Leu-Gln-Ala-Leu-Leu-Arg-Asp-Gln-NH_2) not only showed high affinity for Id1 but also exhibited antiproliferative effects in HT-29 and MCF-7 cancer cells; the IC_{50} value of 3C was determined as 25 μM in both cells. The percentage of sub-G1 in the cell cycle of the cancer cells treated with 5 μM of 3C was increased, indicating the induced apoptosis of cancer cells by 3C. Taken together, the peptide 3C is a promising lead compound for the development of antiproliferative agents.

Keywords: Id1; MyoD; bHLH family; peptide; surface plasmon resonance; circular dicroism; proliferation; cell cycle; antiproliferative agents

Introduction

Id (the inhibitor of DNA-binding proteins or the inhibitor of differentiation) plays important role in the cell growth [1–6], differentiation [7–9], cell cycle control [10,11], and tumorigenesis [7–9,12]. Thus, it has been the potential target for cancer intervention [7,9,11,13–16].

The Id proteins act as negative regulators of transcription factors within the basic helix–loop–helix (bHLH) family, which play an important role in cellular development, proliferation, and differentiation. bHLH proteins such as MyoD contain a DNA-binding motif which contain a cluster of amino acids rich in basic residues and a dimerization motif comprised of the helix–loop–helix (HLH) domain. The Id proteins contain a HLH dimerization motif but lack a basic DNA-binding motif, and Ids could associate with members of the bHLH proteins family through their HLH motif to form high-affinity heterodimers [17,18], thereby preventing bHLH proteins from binding to DNA and inhibiting the transcription of differentiation-associated genes.

The four members of the Id family (Id1–4) have similar amino acids sequences but are subdivided with respect to expression patterns in embryo [19,20]. Id1, the first Id protein, was named for its ability to inhibit the DNA binding of bHLH transcription factors. The associations of Id1 with E proteins and Ets proteins [21,22] have important implications with regards to the role of Id1 in cell cycle progression [10,11] and tumorgenesis [7–9,12]. Id1 also plays an important role in the growth of tumor cells [1–4,6], making it an excellent target for the design of antitumor drugs.

Ids are frequently upregulated in human cancer, and their presence correlates to the proliferation, invasiveness, and neoangiogenesis [14,23]; therefore, Ids are considered as potentially versatile therapeutic targets. Recently, a peptide-conjugated Id1 antisense oligonucleotide homed to tumor endothelium was reported, which can inhibit the tumor growth and metastasis in two different murine models [24]. However, the impact of Id inhibition in human cancer cell lines is not fully assessed.

The goal of this study is to interrupt the interactions among Id1, MyoD, and other DNA-binding proteins such as tumor suppressor-related bHLH transcription factors and to inhibit the proliferation of cancer cells. We selected MyoD as our target to design a

* *Correspondence to: Feng-Di T. Lung, Department of Chemistry, Tunghai University, Taichung, Taiwan, ROC. E-mail: fdlung@thu.edu.tw*

a *Department of Chemistry, Tunghai University, Taichung, Taiwan, ROC*

b *Graduate Institute of Pharmaceutical Chemistry, China Medical University, Taichung, Taiwan, ROC*

‡ *Authors contributed equally to this project.*

series of peptide fragments of MyoD for the development of potent antiproliferative peptide analogs. Binding affinity of each peptide for Id1 was analyzed by surface plasmon resonance (SPR) technology developed with the BIAcore Biosensor. The secondary structure of each peptide was analyzed by circular dichroism (CD) spectroscopy. Effects of peptides in several cancer cells, including breast cancer cells (MCF-7 and MDA MB-231), colon cancer cells (HT-29 and HCT116), leukemia cells (HL-60), hepatoma cells (Hep 3B), non-small-lung cancer cells (NCI-H226), and renal cancer cells (A498), were evaluated by *in vitro* biological assays to investigate the selectivity of each peptide for the tested cancer cells.

Materials and Methods

Materials

All N_{α}-Fmoc derivatives of standard amino acids, Rink amide AM resin [4-(2′,4′-dimethoxyphenyl)-Fmoc-aminomethyl-phenoxy-acetamido-norleucyl aminomethyl resin], and coupling reagents for solid phase synthesis were purchased from Anaspec Inc. (San Jose, CA, USA). DIEA, piperidine and TFA were purchased from Sigma (St Louis, MO, USA). DMF and acetonitrile (HPLC grade) were purchased from Tedia Company (Fairfield, OH, USA). Purification of each peptide was performed by using semi-preparative scale RP-HPLC on a C_{18} column (244 × 10 mm, particle size 10 μm; Lichrospher 100 RP-18, Merck). Human Id1 was provided by Biocheck Inc. (Foster City, CA, USA). All the material reagents for performing BIAcore 3000 biosensor including theSPR, CM5 sensor chip, HBS (Hepes-buffered saline; 10 mM Hepes, pH 7.4, 150 mM NaCl, 3.4 mM EDTA, 0.005% Surfactant P-20), BIAcore 3000 and the BIAevaluation software were purchased from Biacore AB, GE Healthcare company (Pollards Wood, UK). The breast cancer cells (MCF-7), colon cancer cells (HT-29 and HCT116), leukemia cells (HL-60), hepatoma cells (Hep 3B), non-small-lung cancer cells (NCI-H226), and renal cancer cells (A498) were obtained from the American Type Culture Collection (ATCC). Culture medium, fetal bovine serum (FBS), and 1% penicillin and streptomycin were purchased from GIBCO/BRL (Grand Island, NY, USA). (3-(4,5-Dimethylthiazol-2-yl)-2,5-diphenyltetrazolium bromide (MTT) cell proliferation kit was obtained from Boehringer Manheim (Indianapolis, IN, USA) and ELISA plate reader was purchased from using Versamax (Sunnyvale, CA, USA). Apoptotic cells were detected by FACS analysis, using FACS Calibur Flow Cytometer, Becton Dickinson Immunocytometry Systems (Mountain View, CA, USA).

Solid Phase Peptide Synthesis of Peptide Fragments of MyoD

Each peptide fragment of MyoD was synthesized manually [25] in our laboratory by the SPPS [26], using Fmoc/tBu chemistry. Briefly, the Rink amide AM resin was swelled in DMF for 10 min at room temperature, followed by the removal of the Fmoc-protecting group on the resin by treatment with 20% piperidine in DMF for 15 min, repeated twice. The N_{α}-Fmoc, side-chain-protected amino acid, Fmoc–Asn(Trt)–OH, was activated by mixing with the coupling reagent, 1-hydroxybenzotriazole/2-(1H-benzotriazoelyl)-tetramethyl-uronium hexafluorophosphate/*N*,*N*-diisopropylethylamine (HOBt/HBTU/DIEA, 1 : 1 : 2), for 5 min and then added to the reaction vessel for coupling with resin at room temperature for 1.5 h. Cycles of removing Fmoc and coupling with the subsequent amino acids were repeated to produce the desired peptide-bound resin. The crude peptide was removed from resin by TFA cleavage, lyophilized, and then purified by RP-HPLC. After purification, the peptides were characterized by MALDI-TOF-MS spectrometry and RP-HPLC.

Analysis of Interactions of Each Peptide with the Immobilized Id1 by a Biosensor

We have reported applications of SPR technology in analyzing the interactions of Grb2-SH2 protein with its peptidic antagonists and in determining the dissociation equilibrium constant (K_D) of each synthetic peptide [25,27,28]. In this study, Id1 was immobilized on the surface of biosensor chip and then the binding interaction of Id1 with each synthetic peptide was analyzed to determine the binding affinity of each peptide for Id1.

The surface of CM5 chip was activated by the addition of 0.1 M NHS/0.4 M EDC (v/v = 1, 35 μl) at the flow rate of 5 μl/min. Id1 (30 μg/ml, 200 μl) was injected for immobilization on the surface of sensor chip. Finally, 35 μl of ethanolamine hydrochloride (0.1 M, pH 8.5) was injected for blocking the activated surface. In this study, purified peptides were diluted into various concentrations with HBS buffer, and each sample was introduced separately onto the Id1-immobilized CM5 chip at the flow rate of 30 μl/min for 3 min. The binding interaction between each peptide and the Id1 was detected and displayed as a sensorgram by plotting the resonance unit (RU) against time, at least, in triplicate. Detected changes of RU represent the association and dissociation of Id1, and the data were analyzed using BIA evaluation software (Biacore AB, Pharmacia, Uppsala, Sweden) to determine the equilibrium constants of each peptide. The dissociation equilibrium constants (K_D) were calculated as the ratio of dissociation (k_d) and association (k_a) rate constants. The K_D of the binding system could also be determined using the Scatchard analysis by plotting RU/(peptide concentration) *vs* RU to yield a linear line with the slope equal to $-1/K_D$. RU is the maximal RU at a given peptide concentration.

Analysis of the Secondary Structure of Each Peptide by CD Spectroscopy

Solutions of four peptide analogs (**3A, 3B, 3C**, and **3D**) were prepared at the same concentration (3.7 μM, in 0.1 M phosphate buffer, pH 7.2). The secondary structures of these peptides were analyzed by CD spectroscopy using Jasco-715 (Jasco Inc., Easton, MD, USA). The CD spectrum of each peptide solution was recorded at room temperature, and for each CD spectrum, two scans were accumulated using a step resolution of 1 nm, a bandwidth of 1 nm, a response time of 2 s, a scan speed of 100 nm/min, and a high sensitivity. The CD spectrum of the buffer was subtracted from that of each peptide to eliminate interferences from the cell, the solvent, or the optical equipment.

Determination of the Cell Viability by Using the Cell Proliferation Assay

The breast cancer cells (MCF-7 and MDA MB-231), colon cancer cells (HT-29 and HCT116), leukemia cells (HL-60), hepatoma cells (Hep 3B), non-small-lung cancer cells (NCI-H226), and renal cancer cells (A498) were obtained from the ATCC. MCF-7 cells were maintained in Dulbecco's modified Eagle's Medium (DMEM) (GIBCO/BRL, NY, USA) with 10% FBS (GIBCO/BRL), 1% penicillin and streptomycin (GIBCO/BRL) at 37 °C, 5% CO_2, HT-29, HCT116, HL-60, Hep 3B, NCI-H226, and A498 cell lines were cultured in RPMI-1640 (GIBCO/BRL, NY, USA) with 5% FBS (GIBCO/BRL), 1% penicillin (100 units/ml) (GIBCO/BRL) and 1% streptomycin (GIBCO/BRL) at 37 °C, 5% CO_2.

Journal of PeptideScience

The inhibitory effect of each peptide on the proliferation of various cancer cells was determined using the MTT assay. Briefly, HCT116, HT-29, Hep 3B, NCI-H226, A498, MDA MB-231, and MCF-7 cells (10^4/well) were loaded into 96-well culture plates. After 24 h, cells were treated with fresh medium containing various concentrations of each peptide for 24 and 48 h. The suspension cells, HL 60 (10^5/well), were seeded into 24-well plates and treated with each peptide for 48 h. The peptide-treated and the control (cancer cells without treatment with any peptides) were washed once with phosphate-buffered saline (PBS) and reacted with the MTT solution (Boehringer Manheim, Indianapolis, IN) at 37 °C for 2 h to produce the formazan salt. Finally, the formazan salt formed in each cultured cells was dissolved in DMSO, and the optical density (OD) value of each solution was measured at 570 nm using an ELISA reader (Versamax, Sunnyvale, CA, USA).

The optical density (OD) value detected for the control was plotted on the *x*-axis, and considered as 100% of viable cancer cells. The OD value detected for the solution from the peptide-treated cells was also plotted on the *x*-axis, designated as proliferation (% control), to demonstrate the effect of each peptide on the viability of the related cancer cells.

The IC_{50} value represents the concentration of a compound/molecule that caused 50% inhibition of certain reaction, such as some biological processes or proliferation of cells. In the MTT assay, we recorded the concentrations of peptides and the proliferation of cancer cells (% control) as the *x*-values and the *y*-values, respectively. Based on these known *x*-values and *y*-values, the IC_{50} value of each peptide can be calculated by using linear regression. The equation is $a + bx$, where: $a = \overline{y} - b\overline{x}$ *and* $b = \sum(x - \overline{x})(y - \overline{y}) / \sum(x - \overline{x})^2$ and where $\overline{x}$ and $\overline{y}$ are the means of the AVERAGE of our known *x*-values and *y*-values, respectively. This formula can be used in Excel's built-in forecasting to calculate the IC_{50} value of our peptide by setting 50% as the *y*-value.

Flow Cytometric Analysis of the DNA Content and the Cell Cycle in Cancer Cells

Apoptotic cells were detected by FACS analysis of nuclear propidium iodide-stained cells. The cells (1×10^6 cells) were grown in 5 ml of DMEM containing 10% FBS for 24 and 48 h in the presence of 5 μM of the peptide **3A**. For flow cytometry analysis, cells were trypsinized and pelleted by centrifugation. After removal of the supernant, the pelleted cells were fixed by slow addition of 5 ml of the PBS solution containing 70% ethanol (it took about 30 min for completion) at −20 °C. The cells in the suspension were then centrifuged to remove the ethanol, and the pellets of cells were washed with PBS twice. The cells were permeabilized and stained by adding 500 μl of propidium iodide solution (50 μg/ml propidium iodide/1% Triton X-100/0.1 mg/ml RNase in PBS) into the cells, and then the treated cells were incubated for 40 min at 37 °C. The stained cells were subjected to cell cycle analysis by using the Modifit cell cycle analysis software developed with a FACSCalibur Flow Cytometer (Becton Dickinson Immunocytometry Systems).

Statistical Analysis

All values shown are means ± SEM. Differences between treated groups and controls were analyzed by one-way ANOVA followed by Dunnett's multiple comparison tests. Differences in cell growth were analyzed by Student's *t*-test. Significance was accepted at $p < 0.05$.

Results

Design and Synthesis of Peptide Fragments of MyoD

Previous studies using electrophoretic mobility shifts assay (EMSA), CD spectroscopy, and sedimentary equilibrium (SE) ultracentrifigation helped to determine the DNA-binding and oligomerization equilibria of Id, MyoD, and E47 motifs [29]. It was found that homodimers of bHLH proteins such as MyoD are known to activate tissue-specific genes. MyoD is a DNA-binding protein capable of specific interactions specifically involved in the HLH domain. The HLH domain of Id has stronger cooperativity and affinity for heterotetramerization with the bHLH of MyoD [29,30], resulting in inhibition of its DNA-binding activity. Our goal is to inhibit the proliferation of cancer cells by interrupting the interactions of Id1 with DNA-binding proteins such as MyoD and E2A and by affecting the transcription and gene expression through the actions of our designed peptides (Figure 1).

Mutagenesis experiments performed with MyoD protein have demonstrated that the bHLH domain of MyoD is required for dimerization and the basic region of MyoD mediates the DNA binding. Because our goal is to inhibit the proliferation of cancer cells through the interruption of binding interactions among MyoD, Id1, and other bHLH proteins, we designed and synthesized three peptide fragments of MyoD (peptides **1A, 2A**, and **3A**) corresponding to the basic region, helix1 motif, and helix2 motif of MyoD, respectively (Figure 2).

The affinity (or binding potency) of each peptide for Id1 was determined by analyzing the sensorgrams obtained by interacting of each peptide with the immobilized Id1 using the SPR technology developed with the biosensor-BIAcore 3000. Results indicated that among the peptides with the same concentration (50 μM), the peptide **3A,** which is the helix2 region within the *C*-terminal amino acid sequence of MyoD, exhibited the highest binding potency to Id1 (Figure 3).

Therefore, we selected the peptide **3A** as our lead compound and designed a series of *N*-terminal truncated peptide analogs of **3A** (Figure 4) to develop smaller and more potent peptides with enhanced binding affinity for Id1 and/or increased antiproliferative effects in cancer cells.

Synthesized peptides were purified by RP-HPLC and characterized by MALDI-TOF-MS spectroscopy (Table 1)

Analysis of Interactions between Each Peptide and the Immobilized Id1 by a Biosensor

The interaction between each peptide and the immobilized Id1 was analyzed using SPR technology. The Id1 protein was immobilized on the sensor chip for monitoring the interaction between each designed peptide and Id1 in real time (Figure 5).

The affinity of each peptide for Id1 was determined as the SPR-derived K_D value (Table 2) that indicates the affinity (or binding potency) of each peptide for Id1.

Among the four peptides, **3A, 3B, 3C**, and **3D**, the peptide **3C** with the lowest K_D value (12.5 μM) exhibited the highest affinity for Id1, while the peptide **3D** (K_D = 367.2 μM) exhibited the lowest affinity for Id1.

Analysis of the Secondary Structure of Each Peptide by CD Spectroscopy

CD spectroscopy was applied to analyze the secondary structure of synthetic peptides **3A, 3B, 3C,** and **3D**. A maximum signal

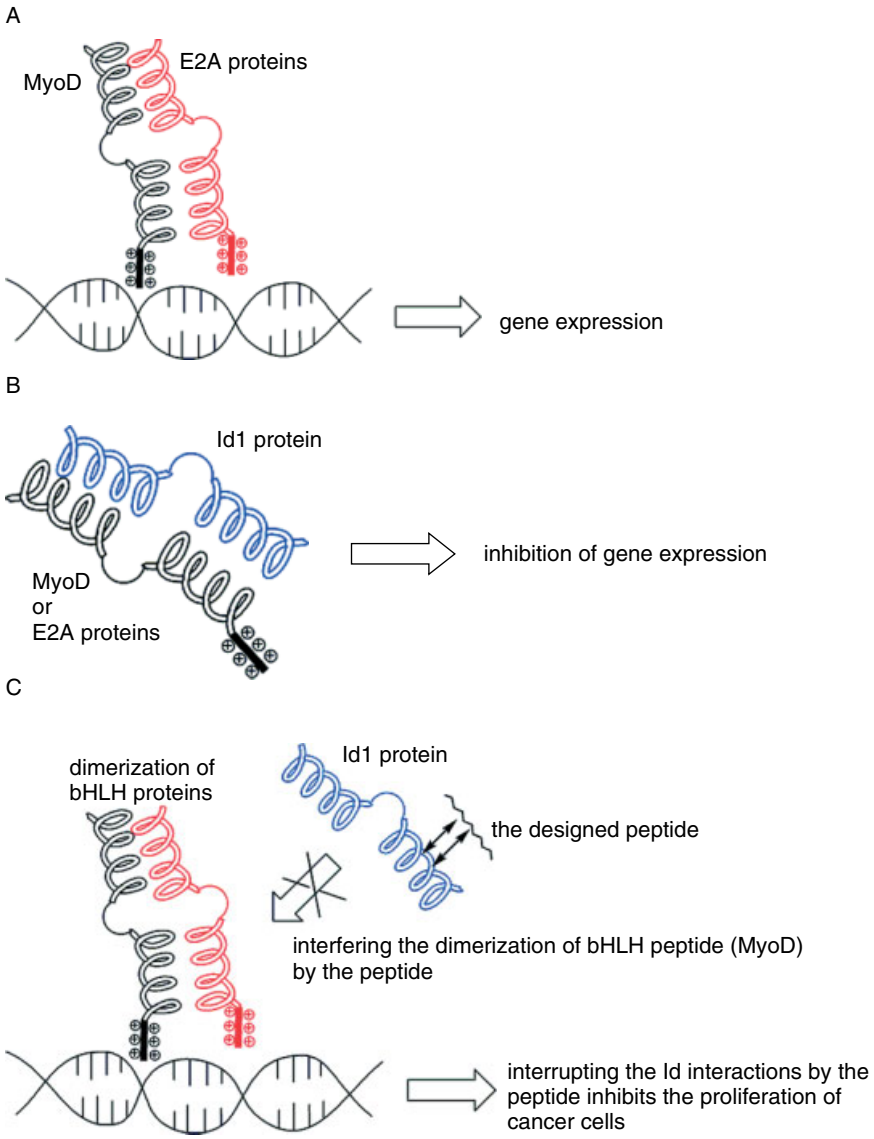

Figure 1. Proposed mechanism of the inhibitory effect of a designed peptide on MyoD-Id1 interactions. (A) A heterodimer of the E2A proteins and MyoD mediates the DNA binding. (B) The inhibitor of DNA-binding protein (Id1) forms the Id1/E2A or Id1/MyoD heterodimer to control the gene expression. Id exerts its dominant negative effect on sequestering the ubiquitously expressed MyoD. (C) Our proposed mechanism for interrupting the Id1 functions by the designed peptide. We propose that the association/interaction of the designed peptide with Id1 should interrupt the binding of Id to bHLH family, leading to the inhibitory effect on the proliferation of cancer cells.

(A)

MyoD

basic region	helix1	loop	helix2
NADRRKAATMRERRR	LSKVNEAFETLKRST	SSNPNQRLP	KVEILRNAIRYIEGLQALLRDQ

(B)

H-Asn-Ala-Asp-Arg-Arg-Lys-Ala-Ala-Thr-Met-Arg-Glu-Arg-Arg-Arg-NH_2 (**1A**)

H-Leu-Ser-Lys-Val-Asn-Glu-Ala-Phe-Glu-Thr-Leu-Lys-Arg-Ser-Thr-NH_2 (**2A**)

H-Lys-Val-Glu-Ile-Leu-Gln-His-Val-Ile-Asp-Tyr-Ile-Glu-Gly-Leu-Gln-Ala-Leu-Leu-Arg-Asp-Gln-NH_2 (**3A**)

Figure 2. Designed peptide fragments of the bHLH (basic helix–loop–helix) domain of MyoD. (A) Amino acid sequences of bHLH domain of MyoD; (B) amino acid sequences of peptides **1A, 2A**, and **3A**.

Journal of PeptideScience

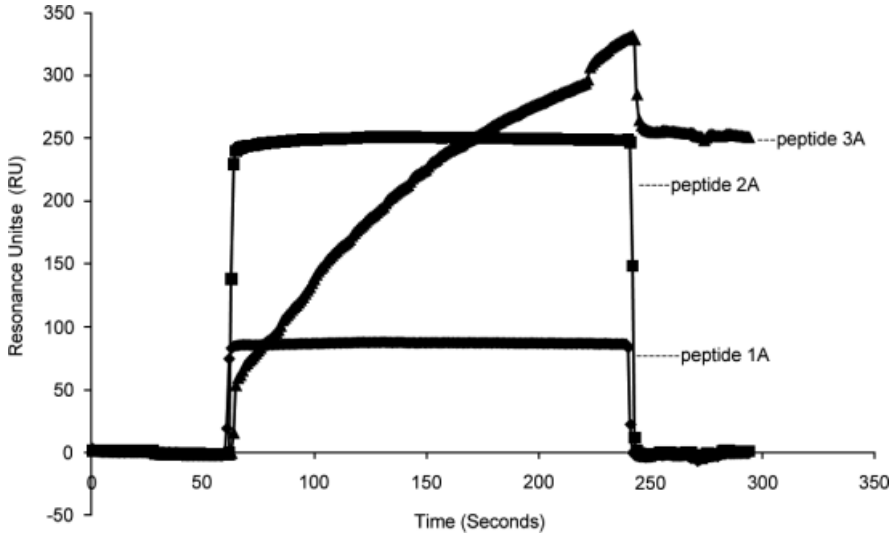

Figure 3. An overlay plot of the binding curves showing the interactions of peptides **1A, 2A** and **3A** with the immobilized Id1. Peptide solutions (50 μM in 10 mM Hepes, 0.5 mM $MnCl_2$, 0.5 M $CaCl_2$, and 0.05% surfactant, pH 7.4) were injected. The bound peptide was dissociated by 30 mM NaCl (20 μl/min).

H-Lys-Val-Glu-Ile-Leu-Gln-His-Val-Ile-Asp-Tyr-Ile-Glu-Gly-Leu-Gln-Ala-Leu-Leu-Arg-Asp-Gln-NH_2 **(3A)**

H-Leu-Gln-His-Val-Ile-Asp-Tyr-Ile-Glu-Gly-Leu-Gln-Ala-Leu-Leu-Arg-Asp-Gln-Cys-NH_2 **(3B)**

H-Tyr-Ile-Glu-Gly-Leu-Gln-Ala-Leu-Leu-Arg-Asp-Gln-Cys-NH_2 **(3C)**

H-Ala-Leu-Leu-Arg-Asp-Gln-NH_2 **(3D)**

Figure 4. Amino acid sequences of designed peptides **3A, 3B,3C**, and **3D**. To synthesize cyclic potent peptide for future structure–activity relationships study, the peptides **3B** and **3C** was designed with an additional Cys at the *C*-terminal of each peptide.

at 190 nm and two minima signals at 203 nm and 221 were characteristics of the peptides **3A, 3B**, and **3C**. Such a CD-spectra pattern has been generally attributed to a partially helical conformation. The contents of α-helix and β-strand presented in these peptides were estimated by using the K2D2 method [31]. Results indicate that the presence of 8.42%, 15.43%, and 8.41% helix were characterized in peptides **3A, 3B,** and **3C,** respectively (Figure 6).

Antiproliferative Effects of Peptides in Various Cancer Cells

The SPR-derived dissociation constant (K_D) of each peptide indicates the potency of each peptide for binding to the Id1 protein, however, it may not reflect the biological effects of peptides in the intact cells because peptides must cross the cell membranes in order to interact with their target proteins. Thus, it is necessary to perform the cell viability assay with peptides to investigate their antiproliferative effects in cancer cells. The dysregulated expression of Id in various human primary tumor biopsies originating from the digestive system, neural tissue, or the reproductive system has been analyzed [13], and the colorectal carcinoma was found to be overexpressed with Id1 [32], thus, the colon cancer cell (HT-29) was the first cancer cell we chose to evaluate the antiprolifeartive effect of our synthetic peptides.

Colon cancer cells (HT-29) were treated with 100 μM of peptides **3A, 3B, 3C**, and **3D** separately for 24 h, and then analyzed by MTT cell viability assay. The formazan product of MTT assay was analyzed for quantification of the viability of cells. Peptide **3A,3B,** and **3C** were found to exhibit significantly inhibitory effect in HT-29 cells (Figure 7A), whereas peptide **3D** enhanced the proliferation of HT-29 cells (the cell viability was increased by additional 60% higher than the control). The peptide **3C** that exhibited the most significant antiproliferative effects in HT-29 cells was served as our lead compound for further biological studies.

To determine the IC_{50} value of peptide **3C,** the HT-29 cells were treated with various concentrations of peptide **3C** (5, 20, 40, 60, and 80 μM) for 24 and 48 h, and then the peptide-treated cells were assayed by MTT assay for the cell viability, proliferation (% of control), as shown in Figure 7B. The IC_{50} of peptide **3C** for 24 and 48 h treated cells were calculated as 27 and 25 μM, respectively.

To study the biological effect of peptide **3C** in breast cancer cells, MCF-7 breast cancer cells were also treated with various

Table 1. Physicochemical characterization of the designed peptides

Peptide	RP-HPLC (Rt, min)	Purity (%)	Theoretical mass (Daltons)	MALDI-TOF-MS (Daltons)
3A	16.35	95	2610.9	2610.9
3B	17.19	96	2244.5	2243.4
3C	17.95	94	1520.7	1521.2
3D	15.5	95	713.7	714.5

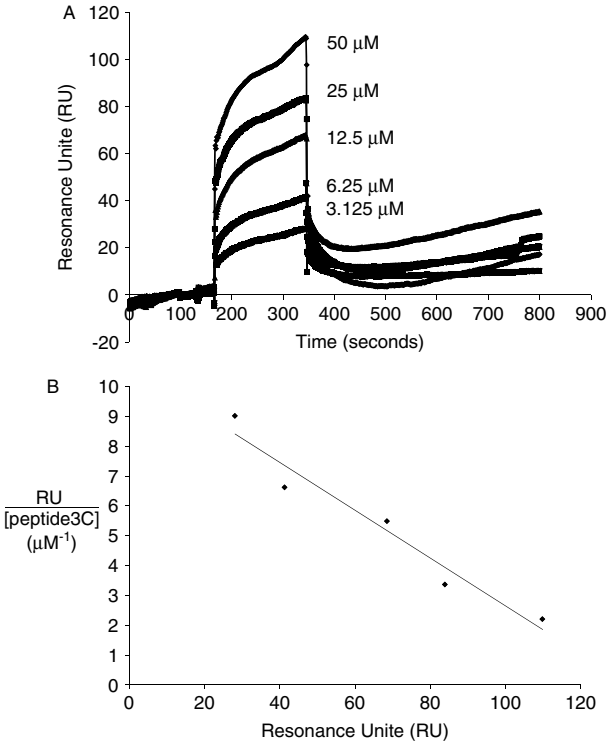

Figure 5. Analysis of binding affinity of the peptide **3C** for the immobilized Id1 using SPR technology. (A) Representative sensorgrams of binding of different concentrations of peptide **3C** (50, 25, 12.5, 6.25, and 3.125 μM) to the immobilized human Id1 which derived from a 1 : 1 binding model. From the global fits k_{on} = 959/ MS and k_{off} = 0.0179/S, and the K_D value was determined as 18.6 μM by using BIA-software. The *x*- and *y*-axes of sensorgram are time (seconds) and RU; (B) scatchard plot of the binding data determined the K_D value as 12.5 μM by plotting the RU/(peptide concentration) *versus* RU, and then calculating the slope which is equal to $-1/K_D$. The *x*- and *y*-axes of plot are RU and RU/(peptide concentration).

Table 2. Equilibrium dissociation constants of the designed peptides

Peptide	K_D[a] (μM)
3A	30.6 ± 7.5
3B	38.4 ± 2.3
3C	12.5 ± 4.6
3D	367.2 ± 19.2

[a] K_D: equilibrium dissociation constant.

concentrations of peptide **3C** (5, 20, 40, 60, and 80 μM) for 24 and 48 h, and then assayed for their viability. The IC_{50} for 24 and 48 h treated MCF-7 cells were calculated as 30 and 25 μM, respectively (Figure 7C).

To investigate the selectivity of peptides for various cancer cells, several cancer cells including leukemia (HL-60), colon cancer (HCT116), hepatoma (Hep 3B), non-small-lung cancer (NCI-H226), and renal cancer (A498) cells were treated separately with peptides **3A** and **3C** for 48 h and then assayed for the cell viability by MTT assay. As summarized in Table 3, the peptide **3A** exhibited antiproliferative effects in leukemia (HL-60) and colon cancer (HCT116) cells (IC_{50} = 30 and 23.9 μM, respectively), and the peptide **3C** also exhibited antiproliferative effects in leukemia

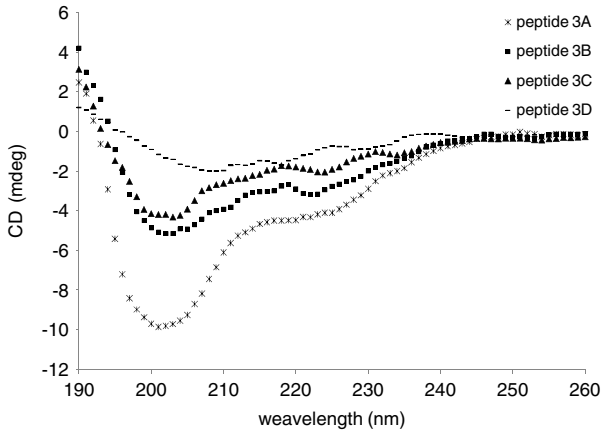

Figure 6. The spectra of the synthesized peptides (**3A, 3B, 3C**, and **3D**) detected by CD spectroscopy.

(HL-60) and colon cancer (HCT116) cells (IC_{50} = 30 and 30 μM, respectively). The IC_{50} value of peptides **3A** and **3C** were higher than 30 μM for hepatoma (Hep 3B), non-small-lung cancer (NCI-H226), and renal cancer (A498) cells. These results suggest that peptides **3A** and **3C** can selectively inhibit the breast cancer cells, leukemia, and colon cancer cells.

The Id1 was demonstrated as a selective mediator of lung metastatic colonization in the triple negative (TN), that is, lacking expression of estrogen receptor and progesterone receptor, and lacking Her2 (human epidermal growth factor receptor 2) amplification, subgroup of human breast cancer. Therefore, we attempted to investigate the inhibitory effect of our most potent peptide **3C** in the invasive cells. MDA MB-231 breast cancer cells (the TN cells) were treated with various concentrations of peptide **3C** (5, 10, 20, 40, 60, and 80 μM) for 24 and 48 h, and the IC_{50} for 24 and 48 h treated cells were determined as 73 and 60 μM, respectively (Figure 8).

In conclusion, our synthetic peptides exhibited antiproliferative effects not only in HT-29 colon cancer cells and MCF-7 breast cancer cells but also in HL-60 leukemia cells and HCT116 colon cancer cells.

For the development of promising anticancer agents, it is important not only to screen the selectivity (or specificity) of **3C** among several cancer cells but also to assay if **3C** exhibited any cytotoxicity in non-cancer cells because Id is not overexpressed in non-cancer cells. Thus, the effect of peptide **3C** on non-cancer cells (human skin cells, HS-68) was tested, and results indicated that the peptides **3C** did not exhibit significant inhibitory effects on the proliferation of HS-68 at the concentrations 25, 50, 75, and 100 μM (Figure 9).

Effects of the Peptide 3C on the DNA Content and the Progression of Cell Cycle

Signals from single cells (size, granularity, or fluorescence) can be measured by flow cytometry as they flow in a fluid stream one by one through a laser point. Flow cytometry data are easy to visualize and to compare between samples. In this study, by staining the cells with nuclear propidium iodide stain, the apoptotic cells can be detected.

Cancer cells treated with peptide **3C** (5 μM) for 24 and 48 h were harvested, and their DNA contents were analyzed by flow cytometry. After 48-h treatment of MCF-7 cells with the peptide

Journal of PeptideScience

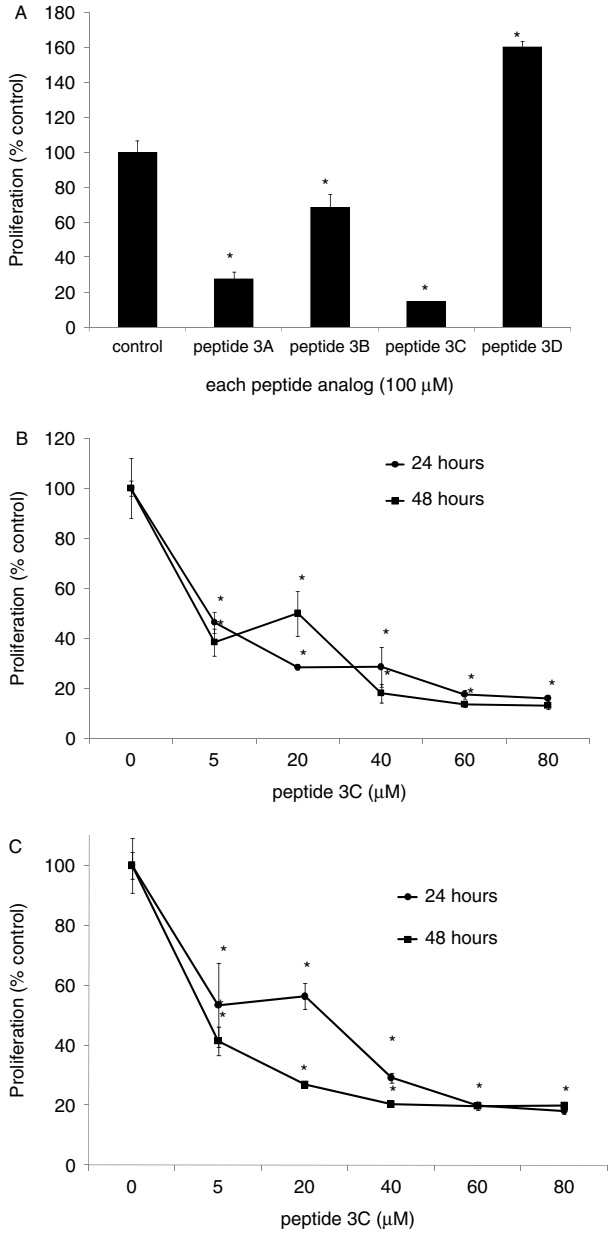

Figure 7. The cell viability of peptide-treated human colon cancer cells and breast cancer cells. (A) Human colon cancer cells HT-29 were treated with 100 μM of peptide **3A, 3B, 3C,** and **3D** for 24 h; (B) human colon cancer cells HT-29 were treated with 5, 20, 40, 60, and 80 μM of **3C** for 24 and 48 h; (C) human breast cancer cells MCF-7 were treated with 5, 20, 40, 60, and 80 μM of **3C** for 24 and 48 h. The cell viability of peptide-treated cancer cells was determined by the MTT assay. Data are the mean value ± SD of three independent experiments. $^{*}p < 0.05$ compared with control.

3C, a pronounced loss of G1 phase cells was found, and the proportion of G1 phase cells decreased from 65.61% to 45.70% (Figure 10A, up)

The proportion of cells in sub-G1 phase increased from 11.82% to 22.13% and from 1.61 to 10.39% for 24 and 48 h peptide-treated cells, respectively (Figure 10A). The percentage of cells in G2/M phase increased markedly from 23.34% to 36.43% after the 48-h incubation. These results are in agreement with the MTT results, indicating that the antiproliferative effect of the peptide **3C** on breast cancer cells was correlated with its induction of the apoptosis of cancer cells. It also demonstrated that the peptide **3C** would arrest at the G2/M phase of the cell cycle in MCF-7 cells.

Discussion

Id proteins play an important role in the generation of blood vessels, the growth of primary, as well as metastatic tumors, thus, we selected Id1 protein as the target for the development of antiproliferative/antitumor agents in this study.

A classic strategy to identify small molecules that specifically target functional Id activities is to use high-throughput screening of large collections of chemical and natural compound libraries, in combination with validated cell-based or cell-free assays. Results of these assays identified the Id associated bHLH partners, including MyoD [33], E2A [34], E47 [35,36], and E proteins [36]. Accordingly, the *in vitro* studies indicated that MyoD directly binds to Id1 [29,30], and there is a stronger affinity between MyoD/Id1 than the affinity between MyoD/E47. More recent *in vivo* investigations demonstrated that the critical interactions are between E2A/Id1 and MyoD/E2A [37]. These studies not only demonstrated the E2A/Id1 interaction is stronger than the MyoD/E2A interaction but also demonstrated the affinity between MyoD/Id1 is stronger than the affinity between MyoD/E2A. Based on these results, we expect that MyoD can associate with Id1 and interrupt interactions involved Id1, therefore, we selected MyoD as our target protein template and designed three peptide fragments of MyoD (Figure 2), which contain the basic, the helix1 and helix2 regions of MyoD to investigate the important region of MyoD for binding to Id1 by the SPR-based method. Our goal is to inhibit the proliferation of cancer cells by interrupting the interactions of Id1 with DNA-binding proteins (Figure 1); however, on the basis of the studies by Lingbeck *et al*. [37], we can not rule out that our designed peptides may not only disrupt the interaction between Id1 and MyoD but also disrupt the interaction between Id1 and E2A.

SPR results demonstrated that peptides **1A, 2A**, and **3A** interacted with the immobilized Id1 but exhibited different binding potency for Id1 and showed significantly different binding profiles (Figure 3). The differences in the association and dissociation phases of the binding curves demonstrated that each peptide exhibited different binding potency for Id1 and the peptide **3A** exhibited the highest binding potency for Id1, indicating the importance of the helix2 region of MyoD (the peptide **3A**) for binding to Id1 (Figure 3). We believe that the helix2 region of MyoD is crucial for associating with Id1 and this result may explain the binding affinity of MyoD for Id1 [33].

Three smaller, *N*-terminal deleted peptide analogs of our lead peptide **3A** (**3B,3C**, and **3D)** were designed (Figure 4), synthesized, and characterized (Table 1) for determining their affinity for Id1 by the SPR technology (Figure 5 and Table 2). It is not surprising that the dissociation constant (K_D) of the most potent peptide **3C** (12.5 μM) is greater than the dissociation constant published for HLH oligomers MyoD/Id (0.7 μM) [29] because the shorter peptide fragments of MyoD may lose some nonconvalent interactions with Id1 due to the deletion of some crucial amino acid residues in MyoD for binding to Id1. Comparing to the numbers of amino acid residues in MyoD protein, there is only 13 amino acid residues in **3C,** but the peptide **3C** still exhibited comparable affinity for Id1 (K_D of MyoD *vs* K_D of **3C**, 0.7 μM *vs* 12.5 μM, respectively), demonstrating the potential of the peptide **3C** as an antagonist of Id1. Thus, the high-affinity peptide **3C** becomes our

Table 3. The inhibitory effects of peptides on the proliferation of human cancer cells

Peptide	IC_{50} (μm)				
	HL-60[a]	HCT116[b]	Hep 3B[c]	H226[d]	A498[e]
3A	30 μM ± 4.1	23.9 μM ± 4.6	>30 μM (81.3 ± 2.6)	>30 μM (64.2 ± 3.7)	>30 μM (82.7 ± 2.6)
3C	30 μM ± 5.5	30 μM ± 2.8	>30 μM (103.4 ± 1.7)	>30 μM (104.9 ± 3.6)	>30 μM (91.3 ± 0.9)

All the cancer cells were treated with the peptides **3A** and **3C** separatively for 48 h, and then their inhibitory effects on the proliferation of the peptide-treated cells were analyzed using the MTT assay. Data are the mean value ± SD of three independent experiments, $p < 0.01$ compared with control.
[a] HL-60, leukemia cells.
[b] HCT116, colon cancer cells.
[c] Hep 3B, hepatoma canaer cells.
[d] NCI-H226, non-small-lung cancer.
[e] A498, renal cancer cells.

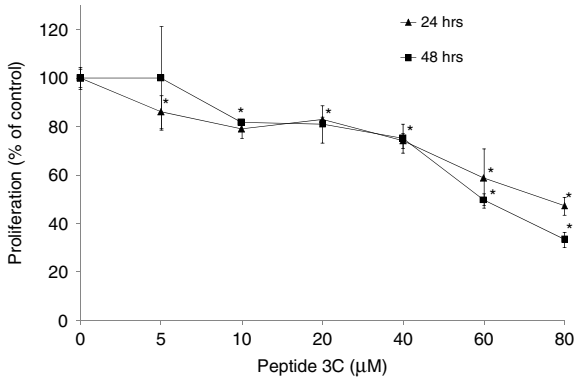

Figure 8. The cell viability of peptide-treated human breast cancer cells. Human breast cancer cells MDA MB-231 were treated with 5, 10, 20, 40, 60, and 80 μM of peptide **3C** for 24 and 48 h. The cell viability was determined by the MTT assay. Data are the mean value ± SD of three independent experiments. $^{*}p < 0.05$ compared with control.

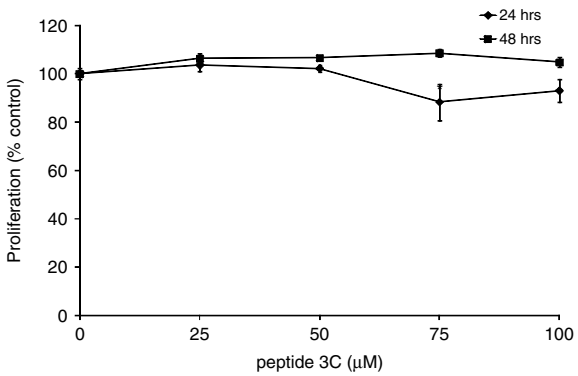

Figure 9. The cell viability of peptide-treated human skin cancer cells. Human skin cells HS-68 were treated with 0, 25, 50, 75, and 100 μM of the peptide **3C** for 24 and 48 h. The cell viability of peptide-treated cells was determined by the MTT assay. Data are the mean value ± SD of three independent experiments.

lead for future design and development of antagonists of Id1 as promising antiproliferative agents by interrupting the Id1-involved interactions.

The SPR-based method established in this study can not only monitor the real-time interaction of each peptide with Id1 but also is useful for screening compounds with high affinity for the immobilized Id1. The SPR-derived K_D value provides an indication of the ability of peptides to bind to Id1 protein *in vitro*, which is informative for further studies of structure-activity relationship; however, this measurement may not reflect their biological effects in the intact cells.

To investigate effects of the secondary structure of each peptide on their affinity for Id1, CD spectroscopy was applied to characterize the conformations of peptides **3A, 3B, 3C,** and **3D** (Figure 6). Results of CD indicate the presence of 8.42%, 15.43%, and 8.41% helix in **3A, 3B,** and **3C,** respectively. These results suggest that the lowest affinity of the peptide **3D** ($K_D = 367.2$ μM) may be due to the absence of the important helical conformation for binding to Id1, and some or all of the first six *N*-terminal amino acid residues of **3C** (Figure 4) are essential for the formation of the helical structure. Although the helical structure is presented in **3A, 3B,** and **3C**, the affinity of each peptide for Id1 ($K_D = 30.6, 38.4,$ and 12.5 μM, respectively) is not correlated with the contents of the helical structures contained in **3A, 3B,** and **3C** (8.42%, 15.43%, and 8.41%, respectively). Comparing the results of SPR-based method with the results of CD spectroscopy, we conclude that the high affinity of **3C** for Id1 is caused by not only the presence of the helical structure but also the presence of the essential amino acid residues for interacting with Id1.

The high affinity of **3C** for Id1 may not reflect its biological effects in the intact cells; therefore, we investigate effects of **3C** in various intact cancer cells by treatment of cancer cells with various concentrations of **3C** and assayed for determination of IC_{50} value of **3C** for the treated-cancer cells (Table 3). The IC_{50} value of **3C** determined in HT-29, MCF-7, HL-60, and HCT116 cancer cells are 25, 25, 30, and 30 μM, respectively, confirming the antiproliferative effects of **3C** in these intact cancer cells.

Results of our assays demonstrate that treatment of human colon or breast cancer cells with peptide **3C** caused decreased viability of both cancer cells in dose-dependent and time-dependent manners. Because previous studies indicated that Id1 was overexpressed in breast cancer and colorectal adenocarcinoma [38–40], we hypothesize that the inhibitory effect of peptide **3C** in the proliferation of both cancer cells may be due to its interruption of the interactions of Id1 protein.

Gupta *et al*. demonstrated that *Id* genes mediate tumor reinitiation and implicate breast cancer lung metastasis [41]. Minni *et al*. identified a set of candidate metastasis genes whose

Journal of PeptideScience

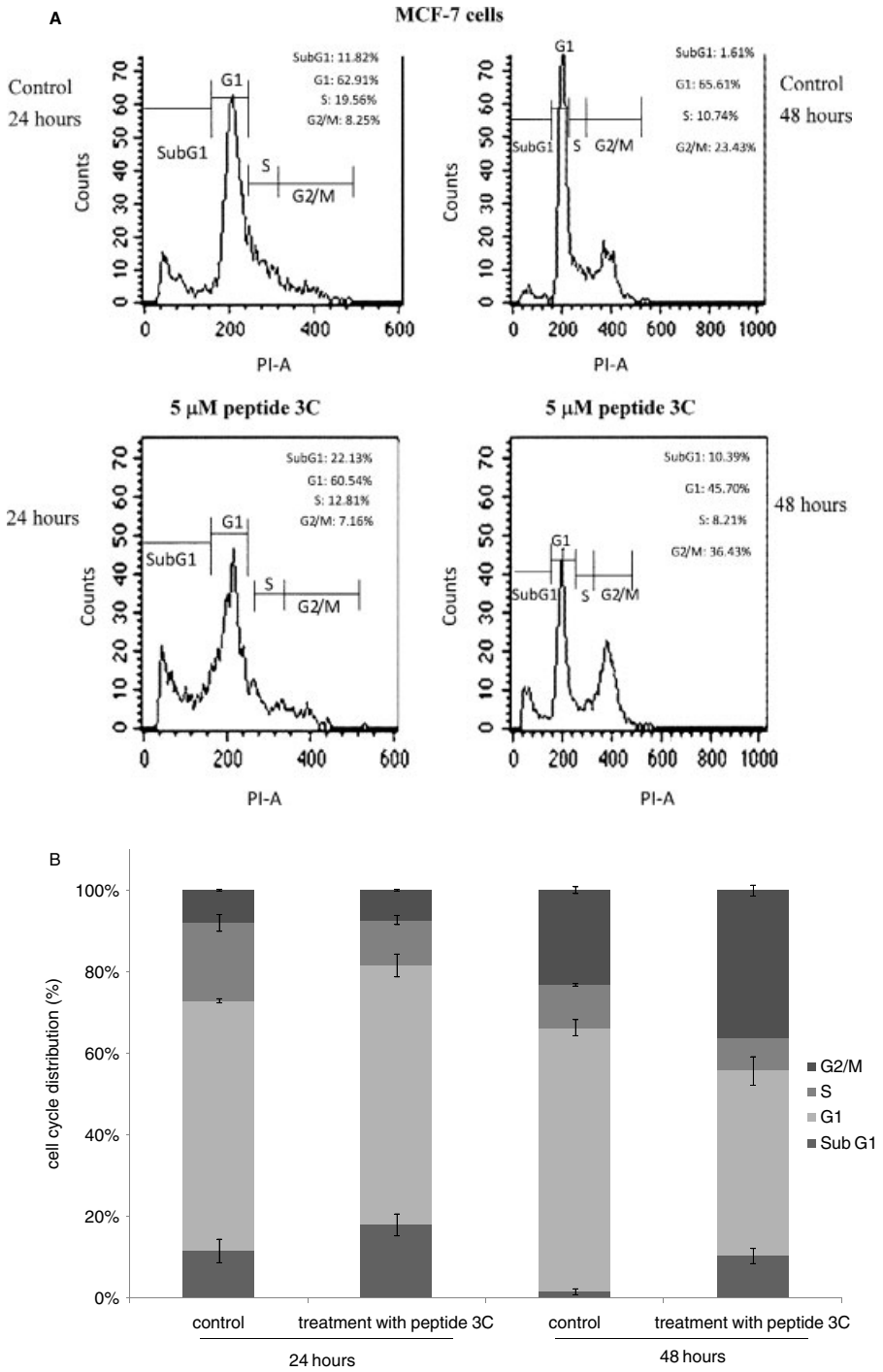

Figure 10. Effects of peptide **3C** on the cell cycle of breast cancer cells (MCF-7). The cells were incubated with 5 μM of peptide **3C** for 24 and 48 h and then analyzed by flow cytometry. (A) The FACS profiles of MCF-7 cancer cells and cancer cells treated with **3C**; (B) effect of **3C** on the distribution of MCF-7 cells in distinct phases in the cell cycle. MCF-7 cells were continuously exposed to **3C** at the indicated concentrations for 24 or 48 h. The graph represents the mean value ± SD of two independent experiments.

expression in primary breast tumors is associated with a high risk of metastasis to the lungs [42], suggested the proliferative mechanisms that initiate metastatic colonization, and implicated Id1 and Id3 as mediators of this malignant function in the TN subgroup of breast cancers. Thus, we investigated the inhibitory effect of **3C** on the proliferation of the invasive cells (lung metastatic MDA MB-231 cells with aggressive Id1 expression) (Figure 8) and found that the IC_{50} of peptide **3C** on TN subgroup invasive cell MDA MB-231 (60 μM, 48 h treatment) were higher than MCF-7 (25 μM, 48 h treatment), HL-60 (30 μM, 48 h treatment), and HCT116 cancer cells (30 μM, 48 h treatment). These results suggested that the peptide **3C** may affect the cell proliferation on overexpressive *Id* gene but lacking expression of estrogen receptor of human breast cancer.

We have demonstrated that our synthetic peptides **3C** exhibited inhibitory effects in the proliferation of HT-29 colon cancer cells and

MCF-7 breast cancer cells. Because the expression of Id proteins in various human primary tumor tissues obtained from biopsies have been analyzed [13] and it was reported that Id1 express particularly on human primary tumors such as colorectal carcinoma and breast cancer cells, we suggest that the antiproiferative effects of peptide **3C** in colon cancer cells and breast cancer cells may be due to the interruption of Id1 protein interactions by **3C**. The peptide **3C** exhibited inhibitory effects not only in the proliferation of HT-29 colon cancer cells and MCF-7 breast cancer cells but also in the proliferation of HL-60 leukemia cells and HCT116 colon cancer cells (Table 3), indicating the selectivity of **3C** for the Id1-overexpressed cancer cells.

To evaluate the potential of **3C** as an antiproliferative agent, we not only screened the selectivity of **3C** among various cancer cells but also assayed the cytotoxicity of **3C** on non-cancer cells (human skin cells, HS-68). Results indicated that even by treatment of HS-68 with 100 μM of peptide **3C** for 24 and 48 h, the inhibitory effect of peptide **3C** on the proliferation of HS-68 cells was not detected (Figure 9), indicating the peptide **3C** exhibited the specificity for cancer cells.

To confirm that the inhibition of proliferation of cancer cells is due to the induced apoptosis of cancer cells instead of necrosis, we analyzed the DNA contents and the apoptotic cells of the peptide **3C**-treated cancer cells by flow cytometry. The peptide **3C**-treated MCF-7 cells showed a decreased G0/G1 phase and an increased sub-G1 peak in the cell cycle (Figure 10), indicating the induction of apoptosis of cancer cells by the treatment of cancer cells with 5 μM of peptide **3C** for 24 and 48 h, and the percentage of cells in G2/M phase increased markedly from 23.34 to 36.43% after incubation for 48 h. These results are in agreement with the MTT results, indicating the antipoliferative effect of **3C** on breast cancer cells was correlated with its induction of apoptosis. It also indicated that the peptide **3C** arrested at the G2/M phase of the cell cycle in MCF-7 cancer cells.

In conclusion, to our knowledge, this work is the first one that reports not only studies of binding interactions between peptide fragments of MyoD and the Id1 protein but also bioassays of effects of peptide analogs in various cancer cells. The peptide **3C** inhibited the proliferation of several cancer cells, and results of the SPR study are in agreement with what we expect; the interactions of Id1 were interrupted by designed peptide analogs. Our findings should provide important insights into the development of antiproliferative agents.

Acknowledgements

This work was supported by the grants from the National Science Council and Taichung Veterans General Hospital, Taiwan, ROC (NSC97-2113-M-029-003 and CVGH-977801). SPR assays were performed by using Biosensor-BIAcore 3000 at the Institute of Biochemistry in National Chung Hsing University (Taichung, Taiwan, ROC). We appreciate our collaborator Dr John Chen at Biocheck Inc. (Foster City, CA, USA) for providing the Id1 protein for this study.

References

1 Barone MV, Pepperkok R, Peverali FA, Philipson L. Id proteins control growth induction in mammalian cells. *Proc. Natl. Acad. Sci. U.S.A.* 1994; **91**: 4985–4988.
2 Hara E, Yamaguchi T, Nojima H, Ide T, Campisi J, Okayama H, Oda K. Id-related genes encoding helix-loop-helix proteins are required for G1 progression and are repressed in senescent human fibroblasts. *J. Biol. Chem.* 1994; **269**: 2139–2145.
3 Lyden D, Young AZ, Zagzag D, Yan W, Gerald W, O'Reilly R, Bader BL, Hynes RO, Zhuang Y, Manova K, Benezra R. Id1 and Id3 are required for neurogenesis, angiogenesis and vascularization of tumour xenografts. *Nature* 1999; **401**: 670–677.
4 Mori S, Nishikawa SI, Yokota Y. Lactation defect in mice lacking the helix-loop-helix inhibitor Id2. *Embo J.* 2000; **19**: 5772–5781.
5 Iavarone A, Garg P, Lasorella A, Hsu J, Israel MA. The helix-loop-helix protein Id-2 enhances cell proliferation and binds to the retinoblastoma protein. *Genes Dev.* 1994; **8**: 1270–1284.
6 Lasorella A, Uo T, Iavarone A. Id proteins at the cross-road of development and cancer. *Oncogene* 2001; **20**: 8326–8333.
7 Norton JD. ID helix-loop-helix proteins in cell growth, differentiation and tumorigenesis. *J. Cell Sci.* 2000; **113**(Pt 22): 3897–3905.
8 Sikder HA, Devlin MK, Dunlap S, Ryu B, Alani RM. Id proteins in cell growth and tumorigenesis. *Cancer Cell* 2003; **3**: 525–530.
9 Coppe JP, Smith AP, Desprez PY. Id proteins in epithelial cells. *Exp. Cell Res.* 2003; **285**: 131–145.
10 Zebedee Z, Hara E. Id proteins in cell cycle control and cellular senescence. *Oncogene* 2001; **20**: 8317–8325.
11 Ruzinova MB, Benezra R. Id proteins in development, cell cycle and cancer. *Trends Cell Biol.* 2003; **13**: 410–418.
12 Alani RM, Hasskarl J, Grace M, Hernandez MC, Israel MA, Munger K. Immortalization of primary human keratinocytes by the helix-loop-helix protein, Id-1. *Proc. Natl. Acad. Sci. U.S.A.* 1999; **96**: 9637–9641.
13 Fong S, Debs RJ, Desprez PY. Id genes and proteins as promising targets in cancer therapy. *Trends Mol. Med.* 2004; **10**: 387–392.
14 Iavarone A, Lasorella A. ID proteins as targets in cancer and tools in neurobiology. *Trends Mol. Med.* 2006; **12**: 588–594.
15 Kim H, Chung H, Kim HJ, Lee JY, Oh MY, Kim Y, Kong G. Id-1 regulates Bcl-2 and Bax expression through p53 and NF-kappaB in MCF-7 breast cancer cells. *Breast Cancer Res. Treat.* 2008; **112**: 287–296.
16 Meteoglu I, Meydan N, Erkus M. Id-1: regulator of EGFR and VEGF and potential target for colorectal cancer therapy. *J. Exp. Clin. Cancer Res.* 2008; **27**: 69.
17 Benezra R, Davis RL, Lockshon D, Turner DL, Weintraub H. The protein Id: a negative regulator of helix-loop-helix DNA binding proteins. *Cell* 1990; **61**: 49–59.
18 Christy BA, Sanders LK, Lau LF, Copeland NG, Jenkins NA, Nathans D. An Id-related helix-loop-helix protein encoded by a growth factor-inducible gene. *Proc. Natl. Acad. Sci. U.S.A.* 1991; **88**: 1815–1819.
19 Jen Y, Manova K, Benezra R. Expression patterns of Id1, Id2, and Id3 are highly related but distinct from that of Id4 during mouse embryogenesis. *Dev. Dyn.* 1996; **207**: 235–252.
20 Jen Y, Manova K, Benezra R. Each member of the Id gene family exhibits a unique expression pattern in mouse gastrulation and neurogenesis. *Dev. Dyn.* 1997; **208**: 92–106.
21 Moldes M, Boizard M, Liepvre XL, Feve B, Dugail I, Pairault J. Functional antagonism between inhibitor of DNA binding (Id) and adipocyte determination and differentiation factor 1/sterol regulatory element-binding protein-1c (ADD1/SREBP-1c) trans-factors for the regulation of fatty acid synthase promoter in adipocytes. *Biochem. J.* 1999; **344**(Pt 3): 873–880.
22 Roberts EC, Deed RW, Inoue T, Norton JD, Sharrocks AD. Id helix-loop-helix proteins antagonize pax transcription factor activity by inhibiting DNA binding. *Mol. Cell. Biol.* 2001; **21**: 524–533.
23 Perk J, Iavarone A, Benezra R. Id family of helix-loop-helix proteins in cancer. *Nat. Rev. Cancer* 2005; **5**: 603–614.
24 Henke E, Perk J, Vider J, de Candia P, Chin Y, Solit DB, Ponomarev V, Cartegni L, Manova K, Rosen N, Benezra R. Peptide-conjugated antisense oligonucleotides for targeted inhibition of a transcriptional regulator in vivo. *Nat. Biotechnol.* 2008; **26**: 91–100.
25 Lung FD, Tsai JY, Wei SY, Cheng JW, Chen C, Li P, Roller PP. Novel peptide inhibitors for Grb2 SH2 domain and their detection by surface plasmon resonance. *J. Pept. Res.* 2002; **60**: 143–149.
26 Merrifield RB. Solid-phase peptide synthesis. *Adv. Enzymol. Relat. Areas Mol. Biol.* 1969; **32**: 221–296.
27 Lung FD, Chen HY, Lin HT. Monitoring bone loss using ELISA and surface plasmon resonance (SPR) technology. *Protein Pept. Lett.* 2003; **10**: 313–319.
28 Lung FD, Tsai JY. Grb2 SH2 domain-binding peptide analogs as potential anticancer agents. *Biopolymers* 2003; **71**: 132–140.
29 Fairman R, Beran-Steed RK, Anthony-Cahill SJ, Lear JD, Stafford WF 3rd, DeGrado WF, Benfield PA, Brenner SL. Multiple oligomeric states

Journal of PeptideScience

regulate the DNA binding of helix-loop-helix peptides. *Proc. Natl. Acad. Sci. U.S.A.* 1993; **90**: 10429–10433.
30 Pesce S, Benezra R. The loop region of the helix-loop-helix protein Id1 is critical for its dominant negative activity. *Mol. Cell. Biol.* 1993; **13**: 7874–7880.
31 Perez-Iratxeta C, Andrade-Navarro MA. K2D2: estimation of protein secondary structure from circular dichroism spectra. *BMC Struct. Biol.* 2008; **8**: 25.
32 Wilson JW, Deed RW, Inoue T, Balzi M, Becciolini A, Faraoni P, Potten CS, Norton JD. Expression of Id helix-loop-helix proteins in colorectal adenocarcinoma correlates with p53 expression and mitotic index. *Cancer Res.* 2001; **61**: 8803–8810.
33 Jan YN, Jan LY. Functional gene cassettes in development. *Proc. Natl. Acad. Sci. U.S.A.* 1993; **90**: 8305–8307.
34 Neuhold LA, Wold B. HLH forced dimers: tethering MyoD to E47 generates a dominant positive myogenic factor insulated from negative regulation by Id. *Cell* 1993; **74**: 1033–1042.
35 Quesenberry PJ, Iscove NN, Cooper C, Brady G, Newburger PE, Stein GS, Stein JS, Reddy GP, Pearson-White S. Expression of basic helix-loop-helix transcription factors in explant hematopoietic progenitors. *J. Cell. Biochem.* 1996; **61**: 478–488.
36 Spicer DB, Rhee J, Cheung WL, Lassar AB. Inhibition of myogenic bHLH and MEF2 transcription factors by the bHLH protein Twist. *Science* 1996; **272**: 1476–1480.
37 Lingbeck JM, Trausch-Azar JS, Ciechanover A, Schwartz AL. In vivo interactions of MyoD, Id1, and E2A proteins determined by acceptor photobleaching fluorescence resonance energy transfer. *FASEB J.* 2008; **22**: 1694–1701.
38 Fong S, Itahana Y, Sumida T, Singh J, Coppe JP, Liu Y, Richards PC, Bennington JL, Lee NM, Debs RJ, Desprez PY. Id-1 as a molecular target in therapy for breast cancer cell invasion and metastasis. *Proc. Natl. Acad. Sci. U.S.A.* 2003; **100**: 13543–13548.
39 Lin CQ, Singh J, Murata K, Itahana Y, Parrinello S, Liang SH, Gillett CE, Campisi J, Desprez PY. A role for Id-1 in the aggressive phenotype and steroid hormone response of human breast cancer cells. *Cancer Res.* 2000; **60**: 1332–1340.
40 Schoppmann SF, Schindl M, Bayer G, Aumayr K, Dienes J, Horvat R, Rudas M, Gnant M, Jakesz R, Birner P. Overexpression of Id-1 is associated with poor clinical outcome in node negative breast cancer. *Int. J. Cancer* 2003; **104**: 677–682.
41 Gupta GP, Perk J, Acharyya S, de Candia P, Mittal V, Todorova-Manova K, Gerald WL, Brogi E, Benezra R, Massague J. ID genes mediate tumor reinitiation during breast cancer lung metastasis. *Proc. Natl. Acad. Sci. U.S.A.* 2007; **104**: 19506–19511.
42 Minn AJ, Gupta GP, Siegel PM, Bos PD, Shu W, Giri DD, Viale A, Olshen AB, Gerald WL, Massague J. Genes that mediate breast cancer metastasis to lung. *Nature* 2005; **436**: 518–524.

